https://doi.org/10.46813/2023-145-153

HIGH RESOLUTION PROBE-FORMING SYSTEM WITH SPHERICAL ABERRATION CORRECTION FOR NUCLEAR MICROPROBE

A.G. Ponomarev, S.V. Kolinko, H.E. Polozhii, V.A. Rebrov
Institute of Applied Physics, National Academy of Sciences of Ukraine, Sumy, Ukraine
E-mail: ponom56@gmail.com

A probe-forming system based on a separate orthomorphic quadruplet of magnetic quadrupole lenses with a short working distance is considered, allowing the system demagnification to be significantly increased. Three magnetic octupole lenses are used to correct spherical aberrations. The parameters of the octupole corrector are calculated using the matricant method. The focusing properties of the system are determined by means of a probe formation optimization process based on the value of the maximum reduced collimated acceptance. The calculations performed showed the feasibility of such a probe forming system for microanalysis and proton beam writing technique.

PACS: 41.85.p; 41.85.Gy; 41.85.Lc

INTRODUCTION

The nuclear scanning microprobe is one of the channels of analytical complexes based on electrostatic accelerators. Currently, the microprobe is widely used for non-destructive microanalysis of samples of various origins [1–4] and proton-beam writing in the fabrication of high-quality 3D micro- and nanostructures [5–7].

The spatial resolution of microprobe setups in the microanalysis mode in techniques such as PIXE, NRA and RBS is at the level of 1 μm, which is due to the high current mode of the focused beam of about 100 pA. Proton beam writing and techniques such as STIM and IBIC are used in low current mode with a beam current of about a few fA, here the resolution reaches the sub-100 nm range. Such spatial resolution parameters are caused by the low brightness of ion sources used in accelerators and not high demagnification of probe-forming systems, which are at the level of 100 [8–11]. Separately, it is worth noting the microprobe setup with demagnifications of 857×130, which is used exclusively for proton-beam writing, in which a resolution of 9×30 nm^2 in the mode of 1000 ions per second is achieved [12]. Improving the resolution for existing microprobe installations by reducing the size of the object collimator leads to a significant decrease in the beam current, and the effect of transparency of the collimator walls does not lead to the desired result.

One of the way to improve the resolution of microprobes is to use high demagnification probe forming systems. However, such systems have very large spherical and chromatic aberrations. If the influence of the latter can be limited by improving the energy spread of the ions in the beam to 10^{-5} [13], then spherical aberrations have to be compensated by a system of octupole lenses. In [14–17] were considered octupole correctors in quadrupole probe-forming systems with low demagnifications, which did not lead to the desired results. Since these systems have low spherical aberrations, reducing them leads to a mismatch between the beam emittance and the acceptance of the probe-forming system and does not increase the focused beam current.

In this paper, we consider a probe-forming system based on a separated orthomorphic quadruplet of magnetic quadrupole lenses, which has the same demagnifications in both transverse directions. Previously, such systems were considered in works [18–21] with a large working distance. By reducing the working distance, a significant increase in demagnifications is achieved, and spherical aberrations are compensated by the use of three magnetic octupole lenses.

1. CALCULATION OF THE OCTUPOLE CORRECTOR PARAMETERS USING THE MATRICANT METHOD

Previously [22] showed that spherical aberrations in quadrupole systems can be completely compensated by three octupole lenses. To calculate the parameters of the octupoles, in this work, the matricant method is used, the general principles of which are described in [23]. The magnetic octupole lens matricant was formed based on the following calculations.

The scalar magnetic potential of the magnetic octupole in the local coordinate system has the form

$$u_m = 4W_4(x^2 - y^2)xy\,. \tag{1}$$

Magnetic field components

$$\begin{aligned} B_x &= -12W_4x^2y + 4W_4y^3\,,\\ B_y &= 12W_4y^2x - 4W_4x^3\,,\\ B_z &= -4W_4'(x^2 - y^2)xy\,. \end{aligned} \tag{2}$$

The trajectory equations of motion of a charged particle in a magnetic field have the form

$$\begin{aligned} x'' &= \frac{e}{p(1+\delta)}\left[-(1+x'^2)B_y + y'(x'B_x + B_z)\right]\sqrt{1+x'^2+y'^2}\,,\\ y'' &= \frac{e}{p(1+\delta)}\left[(1+y'^2)B_x - x'(y'B_y + B_z)\right]\sqrt{1+x'^2+y'^2}\,. \end{aligned} \tag{3}$$

For the subspace of phase moments in the form

$$\begin{aligned} \Phi_x &= \{x,x',x\delta,x'\delta,x^3,x^2x',xx'^2,x'^3,xy^2,xyy',xy'^2,x'y^2,x'yy',x'y'^2\}^{\mathrm{T}}\\ \Phi_y &= \{y,y',y\delta,y'\delta,y^3,y^2y',yy'^2,y'^3,yx^2,yxx',yx'^2,y'x^2,y'xx',y'x'^2\}^{\mathrm{T}} \end{aligned} \tag{4}$$

equations of motion (3) are transformed to the form

$$x'' = \frac{4eW_4}{p}(x^2 - 3y^2)x,$$
$$y'' = \frac{4eW_4}{p}(y^2 - 3x^2)y, \quad (5)$$

where e is the elementary charge;

$p = \sqrt{2MZe\varphi + (Ze\varphi / c)^2}$ is a relativistic momentum;

M is the ion mass; Z is the charge number; φ is the accelerating potential; c is the speed of light.

The procedure of immersion (5) in (4) according to octupole symmetry gives the system of differential equations

$$\frac{d\Phi_{x(y)}}{dz} = P\Phi_{x(y)}, \quad (6)$$

where

$$P(z) = \begin{bmatrix}
0 & 1 & 0 & 0 & 0 & 0 & 0 & 0 & 0 & 0 & 0 & 0 & 0 & 0 \\
0 & 0 & 0 & 0 & -\beta(z) & 0 & 0 & 0 & 3\beta(z) & 0 & 0 & 0 & 0 & 0 \\
0 & 0 & 0 & 1 & 0 & 0 & 0 & 0 & 0 & 0 & 0 & 0 & 0 & 0 \\
0 & 0 & 0 & 0 & 0 & 0 & 0 & 0 & 0 & 0 & 0 & 0 & 0 & 0 \\
0 & 0 & 0 & 0 & 0 & 3 & 0 & 0 & 0 & 0 & 0 & 0 & 0 & 0 \\
0 & 0 & 0 & 0 & 0 & 0 & 2 & 0 & 0 & 0 & 0 & 0 & 0 & 0 \\
0 & 0 & 0 & 0 & 0 & 0 & 0 & 1 & 0 & 0 & 0 & 0 & 0 & 0 \\
0 & 0 & 0 & 0 & 0 & 0 & 0 & 0 & 0 & 0 & 0 & 0 & 0 & 0 \\
0 & 0 & 0 & 0 & 0 & 0 & 0 & 0 & 0 & 2 & 0 & 1 & 0 & 0 \\
0 & 0 & 0 & 0 & 0 & 0 & 0 & 0 & 0 & 0 & 1 & 0 & 1 & 0 \\
0 & 0 & 0 & 0 & 0 & 0 & 0 & 0 & 0 & 0 & 0 & 0 & 0 & 1 \\
0 & 0 & 0 & 0 & 0 & 0 & 0 & 0 & 0 & 0 & 0 & 0 & 2 & 0 \\
0 & 0 & 0 & 0 & 0 & 0 & 0 & 0 & 0 & 0 & 0 & 0 & 0 & 1 \\
0 & 0 & 0 & 0 & 0 & 0 & 0 & 0 & 0 & 0 & 0 & 0 & 0 & 0
\end{bmatrix}$$

$\beta = 4eW_4 / p = eB_{pO} / (pr_{aO}^3)$.

B_{pO} is the induction at the pole of a magnetic octupole, r_{aO} is the octupole aperture radius.

The equation for the matricant of an octupole has a similar form

$$\frac{d\Re_O}{dz} = P\Re_O. \quad (7)$$

The matricant for a rectangular field model of a magnetic octupole lens has the form

$$\Re_O(z) = \begin{bmatrix}
1 & \tau & 0 & 0 & \tau^2\beta/2 & \tau^3\beta/2 & \tau^4\beta/4 & \tau^5\beta/20 & -3\tau^2\beta/2 \\
0 & 1 & 0 & 0 & \tau\beta & 3\tau^2\beta/2 & \tau^3\beta & \tau^4\beta/4 & -3\tau\beta \\
0 & 0 & 1 & \tau & 0 & 0 & 0 & 0 & 0 \\
0 & 0 & 0 & 1 & 0 & 0 & 0 & 0 & 0 \\
0 & 0 & 0 & 0 & 1 & 3\tau & 3\tau^2 & \tau^3 & 0 \\
0 & 0 & 0 & 0 & 0 & 1 & 2\tau & \tau^2 & 0 \\
0 & 0 & 0 & 0 & 0 & 0 & 1 & \tau & 0 \\
0 & 0 & 0 & 0 & 0 & 0 & 0 & 1 & 0 \\
0 & 0 & 0 & 0 & 0 & 0 & 0 & 0 & 1 \\
0 & 0 & 0 & 0 & 0 & 0 & 0 & 0 & 0 \\
0 & 0 & 0 & 0 & 0 & 0 & 0 & 0 & 0 \\
0 & 0 & 0 & 0 & 0 & 0 & 0 & 0 & 0 \\
0 & 0 & 0 & 0 & 0 & 0 & 0 & 0 & 0 \\
0 & 0 & 0 & 0 & 0 & 0 & 0 & 0 & 0
\end{bmatrix}$$

$$\begin{bmatrix}
-\tau^3\beta & -\tau^4\beta/4 & -\tau^3\beta/2 & -\tau^4\beta/2 & -3\tau^5\beta/20 \\
-3\tau^2\beta & -\tau^3\beta & -3\tau^2\beta/2 & -2\tau^3\beta & -3\tau^4\beta/4 \\
0 & 0 & 0 & 0 & 0 \\
0 & 0 & 0 & 0 & 0 \\
0 & 0 & 0 & 0 & 0 \\
0 & 0 & 0 & 0 & 0 \\
0 & 0 & 0 & 0 & 0 \\
0 & 0 & 0 & 0 & 0 \\
2\tau & \tau^2 & \tau & 2\tau^2 & \tau^3 \\
1 & \tau & 0 & \tau & \tau^2 \\
0 & 1 & 0 & 0 & \tau \\
0 & 0 & 1 & 2\tau & \tau^2 \\
0 & 0 & 0 & 1 & \tau \\
0 & 0 & 0 & 0 & 1
\end{bmatrix} \quad (8)$$

where $\tau = z - z_0$, z_0 is the coordinate of the beginning of the effective boundary of the octupole field, for the whole lens $\tau = L_{eff}$, L_{eff} is the effective octupole length.

The complete matricant of the object-target transformation of coordinates of the phase moments is constructed as a result of multiplying the elementary matricant of each optical element, including drift gaps, quadrupole and octupole lenses. Matricants of magnetic quadrupole lenses and drift gaps can be found in [23]. The elements of the full matricant responsible for spherical aberrations depend linearly on the excitations of the octupole lenses. Then we can write the expression for the values of the magnetic induction at the poles of the octupoles in the form

$$\mathbf{A}\cdot\mathbf{b}+\boldsymbol{\gamma}=\boldsymbol{\tau},$$

where $\tau_1 = \Re x_{1,8}$, $\tau_2 = \Re x_{1,14}$ $\tau_3 = \Re y_{1,8}$ are the spherical aberrations, $\Re x, \Re y$ are a full matricants object-target transformations of the phase moments coordinates (4), $\mathbf{b}$ is the vector of unknown values of the magnetic induction at the poles of the octupoles, at which $\boldsymbol{\tau}=0$.

Here matrix $\mathbf{A}$ and vector $\boldsymbol{\gamma}$ are implicitly defined, which are calculated according to the following procedure by varying the magnetic induction of each octupole

$$\begin{aligned} a_{i1}b_1^{(1)} + a_{i2}b_2^{(1)} + a_{i3}b_3^{(1)} + \gamma_i &= \tau_i^{(1,1)} \\ a_{i1}b_1^{(2)} + a_{i2}b_2^{(1)} + a_{i3}b_3^{(1)} + \gamma_i &= \tau_i^{(2,1)} \end{aligned}, \quad i=1,...,3.$$

Then from two equalities one can obtain explicit expressions for the elements of the matrix $\mathbf{A}$ and the vector $\boldsymbol{\gamma}$

$$a_{i1} = \frac{\tau_i^{(2,1)} - \tau_i^{(1,1)}}{b_1^{(2)} - b_1^{(1)}}, \; a_{i2} = \frac{\tau_i^{(2,2)} - \tau_i^{(1,2)}}{b_2^{(2)} - b_2^{(1)}}, \; a_{i3} = \frac{\tau_i^{(2,3)} - \tau_i^{(1,3)}}{b_3^{(2)} - b_3^{(1)}},$$

$$\gamma_i = \tau_i^{(1,1)} - (a_{i1}b_1^{(1)} + a_{i2}b_2^{(1)} + a_{i3}b_3^{(1)}).$$

The vector of unknown values of magnetic induction at the poles of three octupoles, at which spherical aberrations are equal to zero, is now determined from the linear equation

$$\mathbf{A}\cdot\mathbf{b}+\boldsymbol{\gamma}=\mathbf{0}.$$

2. PROBE-FORMING SYSTEM ON THE BASE OF ORTOMORPHIC QUADRUPLET

Fig. 1 shows the layout of magnetic quadrupole and octupole lenses in the probe-forming system.

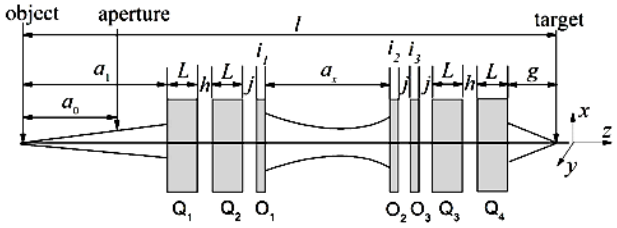

Fig. 1. Layout of magnetic quadrupole and octupole lenses in a probe-forming system with spherical aberration correction

An orthomorphic quadruplet was chosen as the probe-forming system due to the fact that it has the same demagnifications in both transverse directions, $D_x=D_y$. This is achieved by powering the quadrupoles from two power supplies in the form C1D2C2D1, where C means that the lens is converging, and D is diverging in the *xOz* plane, the number indicates which of the two supplies the lens is connected to. The increase in demagnification is affected by the geometric parameters of the quadruplet: the length of the system l, the location of the first doublet relative to the second one a_x (for $a_x>>h$, the quadruplet is called separated and has intermediate crossovers in both transverse directions) and the working distance *g*. In [24] it was shown that an orthomorphic quadruplet has the largest demagnification at *g*=4 cm. The remaining geometric parameters of the probe-forming system have the following values: $a_0=a_1$=800 cm, a_x=140 cm, effective field length of quadrupoles *L*=10 cm, octupoles $i_1=i_2=i_3$=2 cm, *h*=4 cm, *j*=1 cm, radius apertures of quadrupoles r_{aQ}=0.65 cm, octupoles r_{aO}=0.85 cm. For such a geometry, the parameters of the probe-forming system without aberration correction at stigmatic focusing are given in Table for a beam energy of 3 MeV.

Parameters of a probe-forming system based on a separated orthomorphic quadruplet of magnetic quadrupole lenses

Magnetic induction at lens poles, T	
B_{1Q}	0.32806630
B_{2Q}	0.125974694
Demagnification	
$D=D_x=D_y$	574
Chromatic aberration, μm/mrad^3	
Cp_x	-8023
Cp_y	-604
Spherical aberration, μm/mrad^3	
$\langle x/x'^3\rangle$	-208866
$\langle x/x'y'^2\rangle$	370472
$\langle y/y'^3\rangle$	14093
$\langle y/y'x'^2\rangle$	370472

Correction of spherical aberrations is provided with the magnitude of the magnetic induction at the poles of the octupoles B_{1O}=0.02792804 T, B_{2O}=0.13491 T, B_{3O}=–0.1234434 T.

The process of microbeam formation on the target was optimized by the method of maximum reduced collimated acceptance of the probe-forming system, which is described in [25]. The reduced acceptance is determined by the value of the phase volume formed by rectangular object and aperture collimators, which can be focused into a spot on a target with fixed dimensions and has the form

$$\alpha=\alpha_x\alpha_y,\quad \alpha_{x(y)}=4r_{x(y)}R_{x(y)}/a_0, \tag{9}$$

where $2r_{x(y)}$, $2R_{x(y)}$ sizes of the object and aperture collimators, respectively.

For a probe-forming system in which spherical aberrations are fully compensated, the object-target phase coordinate transformation has the form

$$\begin{aligned} x_t &= x_o/D+Cp_x x'_o\delta,\\ y_t &= y_o/D+Cp_y y'_o\delta, \end{aligned} \tag{10}$$

where x_t,y_t are the ion coordinates in the target plane, x_o, y_o, x'_o, y'_o are the phase coordinates of the ion in the object plane, *D* is the demagnification, Cp_x,Cp_y are the chromatic aberrations, δ is the momentum spread.

For the limit trajectory (10) can be written as

$$0.5d=r_{x(y)}/D+Cp_{x(y)}(R_{x(y)}+r_{x(y)})\delta/a_0, \tag{11}$$

where *d* is the size of the square beam spot on the target.

Taking into account (11), we can write the expression for the reduced collimated acceptance

$$\alpha_{x(y)}=4r_{x(y)}(0.5d-r_{x(y)}(1/D-Cp_{x(y)}\delta/a_0))/Cp_{x(y)}\delta. \tag{12}$$

From the condition of maximum collimated acceptance, we obtain

$$r^*=\frac{0.5d}{2(1/D+Cp_{x(y)}\delta/a_0)}\cdot \tag{13}$$

The final expression for the reduced collimated acceptance is

$$\alpha_{x(y)}=\frac{d^2}{4(1/D+Cp_{x(y)}\delta/a_0)Cp_{x(y)}\delta}\cdot \tag{14}$$

Based on (13), the dependence of the size of the object collimator on the size of the spot of the focused beam on the target is shown in Fig. 2, which shows that the sizes are within acceptable limits.

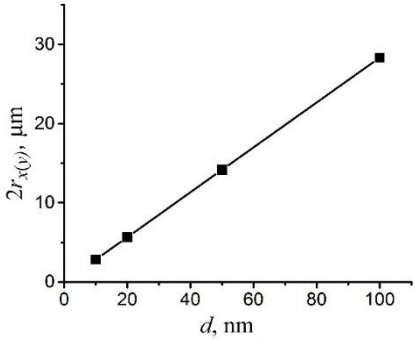

Fig. 2. Dependence of the size of the object collimator on the size of the focused beam on the target

The value of the current of the focused beam on the target depending on the size of the spot is shown in Fig. 3, where the beam current was determined from the expression $I=b\alpha$, here the beam brightness at an energy of 3 MeV is b=100 pA/(μm^2·mrad^2), and the collimated acceptance was calculated from (9), (14). This figure shows that the beam current is within acceptable limits for microanalysis and proton beam writing applications.

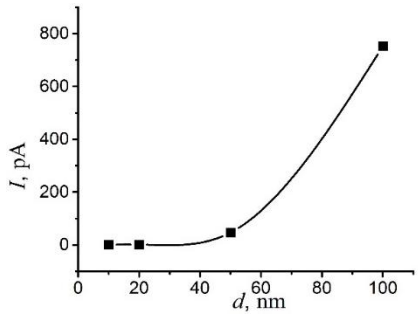

Fig. 3. Dependence of the focused beam current on its size on the target

3. CONCLUSIONS

A probe-forming system based on a separated orthomorphic quadruplet of magnetic quadrupole lenses with a small working distance is considered. This allowed the system demagnification to be increased to 564. Such a system has very large spherical aberrations, making it unacceptable for use. One way of improving the ion-optical characteristics of such a system is to correct spherical aberrations using three magnetic octupole lenses. The approach developed to correct aberrations using the matricant method allowed the parameters of the octupoles to be determined. Optimization of the microprobe formation process using the value of the maximum reduced collimated acceptance allowed to determine the size of the object collimator and the value of the focused beam current for the probe size in the range of 10…100 nm, which shows the feasibility of such a system for various applications.

ACKNOWLEDGEMENT

This work was carried out within the framework of the state program of Ukraine "Research and development in the field of physical and mathematical sciences". State registration number 0120U101035.

REFERENCES

1. C.G. Ryan. PIXE and the nuclear microprobe: Tools for quantitative imaging of complex natural materials // *Nucl. Instr. Meth. Phys. Res., Sect. B.* 2011, №269, p. 2151-2162.
2. M.B.H. Breese, D.N. Jamieson, P.J.C. King. *Materials Analysis using a Nuclear Microprobe*. New York: John Wiley and Sons Inc., 1996, 428 p.
3. A.A. Valter, K.B. Knight, G.K. Eremenko, D.V. Magilin, A.A. Ponomarov, A.I. Pisansky A.V. Romanenko, A.G. Ponomarev. Spatial investigation of some uranium minerals using nuclear microprobe // *Physics and Chemistry of Minerals*. 2018, №45, p. 533-547.
4. O. Romanenko, V. Havranek, A. Mackova, M. Davidkova, M. Cutroneo, A.G. Ponomarev, G. Nagy, J. Stammers. Performance and application of heavy ion nuclear microbeam facility at the Nuclear Physics Institute in Řež, Czech Republic // *Review of Scientific Instruments*. 2019, v. 90, N 1, p. 013701 (p. 11).
5. F. Watt, M.B.H. Breese, A. Bettiol, J.A. van Kan. Proton beam writing: review // *Materials today*. 2007, v. 10, N 6, p. 20-29.
6. I. Rajta, S.Z. Szilasi, P. Fürjes, Z. Fekete, Cs. Dücso. Si micro-turbine by proton beam writing and porous silicon micromachining // *Nucl. Instr. Meth. Phys. Res., Sect. B*. 2009, №267, p. 2292-2295.
7. H.E. Polozhii, A.G. Ponomarev, S.V. Kolinko, V.A. Rebrov. Vector proton beam writing system // *Problems of Atomic Science and Technology*. 2022, №3, p. 52-55.
8. F. Watt, J.A. van Kan, I. Rajta, A.A. Bettiol, T.F. Choo, M.B.H. Breese, T. Osipowicz. The National University of Singapore high energy ion nano-probe facility: Performance tests // *Nucl. Instr. Meth. Phys. Res., Sect. B.* 2003, №210, p. 14-20.
9. M. Rothermel, T. Butz, T. Reinert. Rearranging a nanoprobe: Line foci, grid shadow patterns and performance tests // *Nucl. Instr. Meth. Phys. Res., Sect. B*. 2009, №267, p. 2017-2020.
10. J. Simicic, P. Pelicon, M. Budnar, Z. Smit. The performance of the Ljubljana ion microprobe // *Nucl. Instr. Meth. Phys. Res., Sect. B*. 2002, №190, p. 283-286.
11. C. G. Ryan, D. N. Jamieson. A high performance quadrupole quintuplet lens system for the CSIRO-GEMOC nuclear microprobe // *Nucl. Instr. Meth. Phys. Res., Sect. B*. 1999, №158, p. 97-106.
12. Y. Yao, J.A. van Kan. Automatic beam focusing in the 2 nd generation PBW line at sub-10 nm line resolution // *Nucl. Instr. Meth. Phys. Res., Sect. B*. 2015, №348, p. 203-208.
13. D.J.W. Mous, R.G. Haitsma, T. Butz, R.H. Flagmeyer, D. Lehmann, J. Vogt. The novel ultrastable HVEE 3.5 MV SingletronTM accelerator for nanoprobe applications // *Nucl. Instr. Meth. Phys. Res., Sect. B*. 1997, №130, p. 31-36.
14. D.N. Jamieson, G.J.F. Legge. The measurement and correction of spherical aberration in a magnetic quadrupole lens system // *Nucl. Instr. Meth. Phys. Res., Sect. B*. 1988, №34, p. 411-422.
15. D.N. Jamieson, G.J.F. Legge. Multipole lenses and their application in nuclear microprobe lens systems // *Nucl. Instr. Meth. Phys. Res., Sect. B*. 1988, №30, p. 235-241.
16. Y. Dou, D.N. Jamieson, J. Liu, L. Li. A high excitation magnetic quadrupole lens quadruplet incorporating a single octupole lens for a low spherical aberration probe forming lens system // *Nucl. Instr. Meth. Phys. Res., Sect. B*. 2018, №419, p. 49-54.
17. M. Rothermel, D. Spemann. Alignment tolerances and octupole aberration corrections in an ion nanoprobe // *Book of abstract 13 International Conference on Nuclear Microprobe Technology and Applications* 22-27 July 2012, Lisbon, Portugal, p. 78.
18. A.G. Ponomarev, K.I. Melnik, V.I. Miroshnichenko. Parametric multiplets of magnetic quadrupole lenses: application prospects for probe-forming systems of nuclear microprobe // *Nucl. Instr. Meth. Phys. Res., Sect. B*. 2005, №231, p. 86-93.
19. A.A. Ponomarova, K.I. Melnik, G.S. Vorobjov, A.G. Ponomarev. One-stage probe-forming systems with quadrupole lenses excited by individual power

supplies // *Nucl. Instr. Meth. Phys. Res., Sect. B*. 2011, №269, p. 2202-2205.
20. S.V. Kolinko, A.G. Ponomarev, V.A. Rebrov. Precise centering and field characterization of magnetic quadrupole lenses // *Nucl. Instr. Meth. Phys. Res., Sect. A*. 2013, №700, p. 70-74.
21. K.I. Melnik, D.V. Magilin, A.G. Ponomarev. Experimental results of microprobe focusing by quadruplet with four independent lens power supplies // *Nucl. Instr. Meth. Phys. Res., Sect. B*. 2013, №306, p. 17-20.
22. O. Scherzer // *Optik*. 1947, №2, p. 114.
23. А.Г. Пономарев, А.А. Пономарев. *Формирование пучков ионов в ядерном сканирующем микрозонде*. Сумы: Коллаж-принт, 2019, 368 с.
24. K.I. Melnik, D.V. Magilin, A.G. Ponomarev. Optimization of the working distance of an ion microprobe-forming system // *Nucl. Instr. Meth. Phys. Res., Sect. B.* 2009, №267, p. 2036-2040.
25. A.G. Ponomarev, A.A. Ponomarov. Beam optics in nuclear microprobe: A review // *Nucl. Instr. Meth. Phys. Res., Sect. B.* 2021, №497, p. 15-23.

Article received 18.04.2023

ЗОНДОФОРМУЮЧА СИСТЕМА ВИСОКОЇ РОЗДІЛЬНОЇ ЗДАТНОСТІ З КОРЕКЦІЄЮ СФЕРИЧНИХ АБЕРАЦІЙ ДЛЯ ЯДЕРНОГО МІКРОЗОНДА

О.Г. Пономарьов, С.В. Колінько, Г.Є. Положій, В.А. Ребров

Розглянуто зондоформуючу систему на базі розподіленого ортоморфного квадруплету магнітних квадрупольних лінз з малою робочою відстанню, що дозволило значно збільшити коефіцієнти зменшення. Для корекції сферичних аберацій застосовуються три магнітні октупольні лінзи. Розрахунок параметрів октупольного коректора виконується методом матрицантів. Фокусуючі властивості системи визначаються за рахунок оптимізації процесу формування зонда на основі величини максимального приведеного колімованого аксептансу. Проведені розрахунки показали, що така система може бути реалізована для застосування в методиках мікроаналізу та протонно-променевої літографії.